Status of the BNL Muon $(g - 2)$ Experiment[*]

R. Prigl (2), H.N. Brown (2), G. Bunce (2), R.M. Carey (1), P. Cushman (8), G.T. Danby (2), P.T. Debevec (7), H. Deng (12), W. Deninger (7), S.K. Dhawan (12), V.P. Druzhinin (9), L. Duong (8), W. Earle (1), E. Efstathiadis (1), F.J.M. Farley (12), G.V. Fedotovich (9), S. Giron (8), F. Gray (7), M. Grosse Perdekamp (12), A. Grossmann (5), U. Haeberlen (6), M. Hare (1), E.S. Hazen (1), D.W. Hertzog (7), V.W. Hughes (12), M. Iwasaki (11), K. Jungmann (5), D. Kawall (12), M. Kawamura (11), B.I. Khazin (9), J. Kindem (8), F. Krienen (1), I. Kronkvist (8), R. Larsen (2), Y.Y. Lee (2), W. Liu (12), I. Logashenko (9), R. McNabb (8), W. Meng (2), J.-L. Mi (2), J.P. Miller (1), W.M. Morse (2), P. Neumayer (5), D. Nikas (2), C.J.G. Onderwater (7), Y. Orlov (3), C. Ozben (2), J. Paley (1), C. Pai (2), C. Polly (7), J. Pretz (12), G. zu Putlitz (5), S.I. Redin (12), O. Rind (1), B.L. Roberts (1), N. Ryskulov (9), S. Sedykh (7), Y.K. Semertzidis (2), Yu.M. Shatunov (9), E. Sichtermann (12), E. Solodov (9), M. Sossong (7), A. Steinmetz (12), L.R. Sulak (1), M. Tanaka (2), C. Timmermans (8), A. Trofimov (1), D. Urner (7), D. Warburton (2), D. Winn (4), A. Yamamoto (10), D. Zimmerman (8).

(1) Department of Physics, Boston University, Boston, MA 02215, USA, (2) Brookhaven National Laboratory, Upton, NY 11973, USA, (3) Newman Laboratory, Cornell University, Ithaca NY 14853, USA, (4) Fairfield University, Fairfield, CT 06430, USA, (5) Physikalisches Institut der Universität Heidelberg, 69120 Heidelberg, Germany, (6) MPI für Med. Forschung, 69120 Heidelberg, Germany, (7) Department of Physics, University of Illinois, Urbana, IL 61820, USA, (8) Department of Physics, University of Minnesota, Minneapolis, MN 55455, USA, (9) Budker Institute of Nuclear Physics, Novosibirsk, Russia, (10) KEK, Japan, (11) Tokyo Institute of Technology, Tokyo, Japan, (12) Department of Physics, Yale University, New Haven, CT 06511, USA.

The muon $(g - 2)$ experiment at Brookhaven has been taking data since 1997. Analyses of the data taken in 1997 and 1998, which include about 2% of the data taken so far, have improved the experimental accuracy in the muon anomalous magnetic moment to $a_{\mu(expt)} = 1165921(5) \times 10^{-9}(4\,ppm)$. The value agrees with standard theory. Analysis of the 1999 data, about 25% of the existing data set, is nearing completion and analysis of the 2000 data has started. The experiment is preparing for another major data taking run, this time storing negative instead of positive muon beams.

Presented at the

5th International Symposium on Radiative Corrections
(RADCOR–2000)
Carmel CA, USA, 11–15 September, 2000

1 Introduction

The Brookhaven g-2 experiment E821 is designed to provide a precision test of the standard model prediction for a_μ which is dominated by the QED radiative corrections but has sizeable contributions from hadronic loops, $a_\mu^{Had} = 6739(67) \times 10^{-11}$ or $57.8(7)\,ppm$ in a_μ, as well as electroweak loops, $a_\mu^{EW} = 1.30(4)\,ppm$. The theory of a_μ is discussed in detail in another contribution to these proceedings [1]. The goal of E821 is to reduce the error in a_μ to $0.35\,ppm$, a fraction of the electroweak contribution.

The experiment measures the muon anomaly a_μ directly rather than the g-factor. Therefore we commonly express contributions and errors in units of a_μ. Any numbers given in ppm here have to be multiplied by $1.165... \times 10^{-9}$ for comparison with the absolute numbers found in [1] and most other theoretical papers on the muon g-factor.

2 The Brookhaven Experiment

The principle of the measurement is similar to the third CERN experiment [2]. Polarized muons are stored in a uniform dipole magnetic field with electrostatic quadrupoles providing weak vertical focussing. The muon spin precesses relative to the momentum vector with the frequency

$$\vec{\omega}_a = -\frac{e}{m_\mu}\left[a_\mu\vec{B} - \left(a_\mu - \frac{1}{\gamma_\mu^2 - 1}\right)\vec{\beta}\times\vec{E}\right], \tag{1}$$

where $\vec{\beta} = \vec{v}/c$, $\gamma = 1/\sqrt{1 - v^2/c^2}$, and assuming that $\frac{E}{c} \ll B$ and $\vec{\beta}\cdot\vec{B} \approx 0$. The dependence of ω_a on the electric field $\vec{E}$ can be eliminated by storing muons with the "magic" γ_μ=29.3, corresponding to a muon momentum $p_\mu = 3.094$ GeV/c. In this ideal case, $a_\mu - 1/(\gamma_\mu^2 - 1) = 0$, and the focussing electric field does not affect the spin precession frequency. a_μ is then extracted from $\omega_a \approx 2\pi \times 230$ kHz through

$$a_\mu = \frac{\omega_a/\omega_{\rm p}}{\mu_\mu/\mu_{\rm p} - \omega_a/\omega_{\rm p}} \tag{2}$$

where $\omega_{\rm p} \approx 2\pi \times 62$ MHz is the free proton precession frequency in the same magnetic field seen by the muons. The ratio of muon to proton magnetic moments is $\mu_\mu/\mu_{\rm p} = 3.18334539(10)$ [3,4].

The source of the stored muons is the Alternating Gradient Synchrotron (AGS) proton beam, which delivers 6-12 bunches with a total of 40-60 $\times$ 10^{12} protons at 24 GeV/c onto a nickel production target every 2.7 s. The individual bunches have a total width of about 100 ns and are spaced apart by 33 ms.

From each bunch about 4×10^7 pions at ≈ 3.1 GeV/c are transported from the target along a 116 m beam line. About 50 % of the pions decay along the transport line and a momentum slit followed by a bending magnet near the downstream end selects either pions or forward decay muons from a slightly higher momentum pion beam for injection
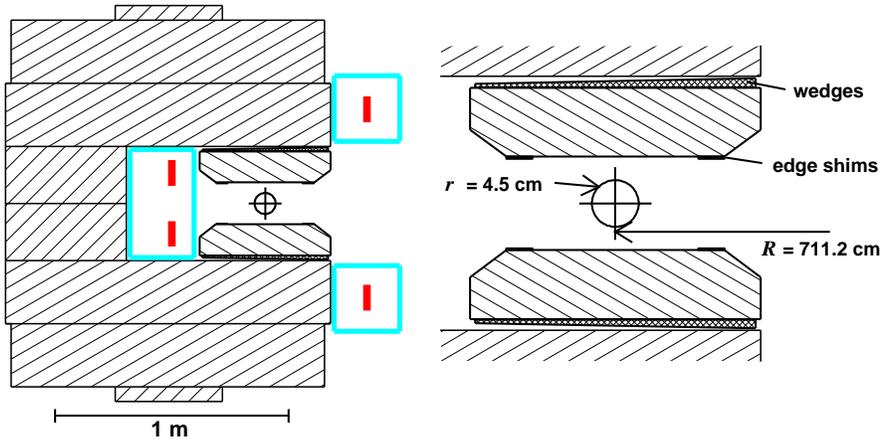
Figure 1: Storage ring magnet cross section and detailed view of the magnet gap region.

into the storage ring. After passing through a hole in the back of the storage ring magnet yoke and a field free region supplied by a superconducting inflector magnet [5], the pion or muon beam enters the toroidal storage region which has a radius of 7.112 m and a 9 cm diameter cross section. The storage ring magnet is described in detail in [6].

One of the major improvements over the last CERN experiment is the use of direct muon injection. In pion injection mode a small fraction of muons from pion decay, $\pi^+ \rightarrow \mu^+ \nu_\mu$, are launched onto a stable orbit and are stored. In muon injection mode, a total kick of ≈ 11 mrad on the first one or two turns is needed to store the muons born in the pion decay channel. The muon kicker is a pulsed magnet consisting of three sections of pairs of current sheets, each 1.7 m long. The peak current through the plates during a 400 ns wide pulse is about 4100 A, providing a vertical field of 0.016 T superimposed on the 1.45 T field of the storage ring magnet.

The continuous superferric 'C'-shaped storage ring magnet, Fig. 1, is excited by superconducting coils which carry a current of 5177 A. The yoke consists of twelve 30 degree sections bolted together at the four corners, with azimuthal gaps of less than 1 mm. The pole pieces are 10 degrees long and aligned with the yoke sectors. The azimuthal gap between adjacent pole pieces of about $75 \, \mu$m is filled with insulating Kapton foils to avoid irregular eddy current effects. The vertical gap between pole and yoke decouples the yoke and pole pieces, which are fabricated from high quality steel, and allows the insertion of iron wedges to compensate for the C-magnet quadrupole. The 10 cm wide wedges are radially adjustable. This allows us to locally change the total air gap and thus the dipole field component for better field homogeneity in azimuth. The four edge shims, 5 cm wide and about 3 mm high, are the main tool for reducing field variations over the beam cross section. Continuous current sheets glued to the pole pieces are used to further reduce the fractional inhomogeneity in the integral field. The gradual improvement of the field integral across the aperture is shown in Fig. 2.

During data taking an array of nuclear magnetic resonance (NMR) probes embedded in the top and bottom plates of the twelve vacuum chambers is used to monitor and
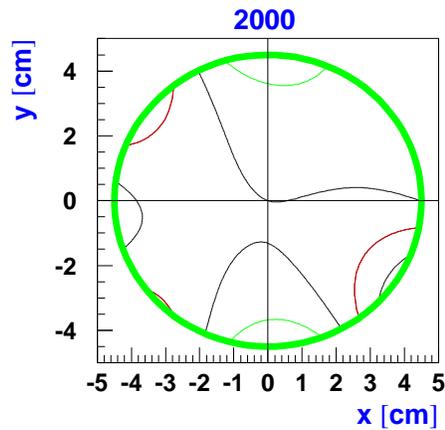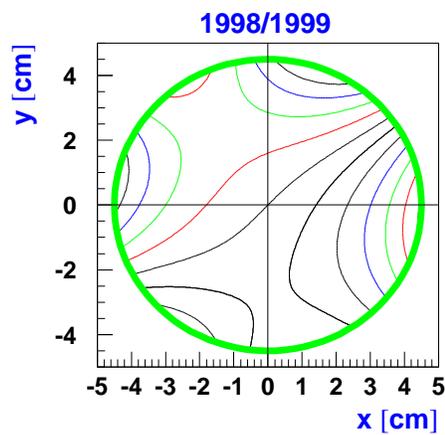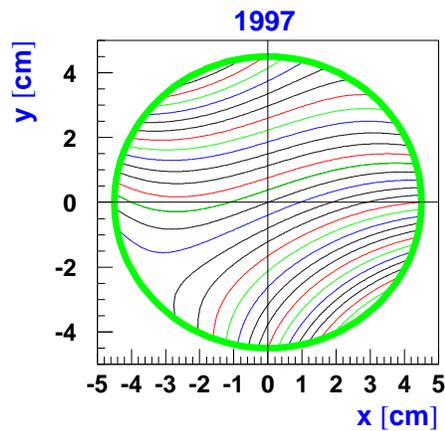
Figure 2: Typical contour plot of the magnetic field integrated over azimuth during the 1997 run (top), 1998 (1999) run (middle), and the 2000 run (bottom). x denotes the radial and y the vertical direction. Each contour line represents a fractional change of 1×10^{-6}. No efforts were made to improve the field quality between the 1998 and 1999 run and the field quality was the same for these runs. The most significant improvement for 2000 came from the installation of a new inflector magnet.

3
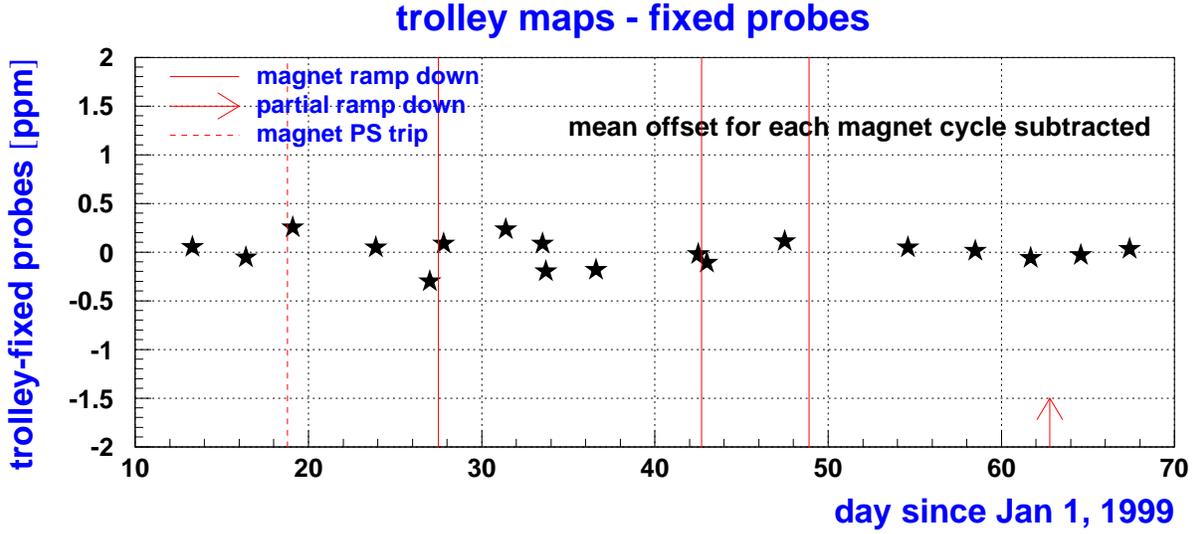
Figure 3: Difference between the field average measured by the trolley and the field average predicted by the monitoring probes. It is assumed that the true difference is constant during each magnet-on period and fluctuations are caused by the limited accuracy of the individual measurements.

stabilize the magnetic field [7]. About one third of the 375 probes installed are typically used in the field analysis. The field inside the storage region is mapped twice a week using a hermetically sealed trolley operating in vacuum and containing a matrix of 17 NMR probes. The probes in the trolley are calibrated in place against a standard probe [8]. The first trolley run in a magnet cycle establishes the offset between the average field measured by the monitoring probes and the average field seen by the muon beam. Subsequent trolley runs can then be used to determine the accuracy of the continuous field "tracking" with the monitoring probes. The quality of the field tracking is shown in Fig. 3 for the 1999 run.

The decay positrons from $\mu^+ \to e^+ \nu_e \overline{\nu}_\mu$, which constitute our signal, range in energy from 0 GeV to 3.1 GeV, and are detected with 24 Pb-scintillating fiber calorimeters placed symmetrically around the inside of the storage ring. Because of the parity violating nature of the weak decay, the high-energy positrons are preferentially emitted along the muon spin direction. The muon spin precession is reflected in the decay positron spectrum, $N(t)$, where we expect

$$N(t) = N_0(E)e^{-t/\tau_\mu} \left[1 - A(E)\cos\left(\omega_a t + \phi\right)\right]. \tag{3}$$

The normalization constant N_0 depends on the energy threshold E as does the asymmetry parameter A. For E=2.0 GeV, A is ≈ 0.4.

The arrival times of the positrons are recorded in multi-hit time-to-digital converters (TDCs), and the calorimeter pulses are also sampled by a 400 MHz waveform digitizer (WFD). A laser and light emitting diode (LED) system are used to monitor potential time

4

and gain shifts. Several detector stations are outfitted with a finely segmented hodoscope array of 20×32 small scintillating elements connected to a multianode phototube, which provide position sensitive information on the muon decay positron. Additional event information is derived from stations equipped with five scintillator paddles oriented horizontally. Finally, a set of wire chambers in one section of the ring provides information on the stored muon phase space by measuring the flight path of the decay electrons and tracing them back to their origin. The distribution of the muon beam across the aperture has to be convoluted with the magnetic field to determine the average field seen by the muons. The mean radial distribution of the stored muons can also be obtained from the fast rotation signal from the initial time structure of the injected beam.

3   Present Status of Results

In the first data taking run of the experiment in 1997 pion injection was used because the muon kicker was still under construction. This mode suffers from a low efficiency - only about 20 muons get stored per 10^6 pions injected into the storage ring - as well as from a significant flash caused by hadronic interactions of pions that do not decay and hit the inflector channel wall at the end of the first turn. The result from this run, $a_\mu = 1\,165\,925(15) \times 10^{-9}$, is discussed in [9]. In 1998 the muon kicker was commissioned and first data were taken in muon injection mode. The run was cut short by a hardware failure in the beamline. The analysis of the 1998 data, most of which taken during the last week of running, resulted in a value of $a_\mu = 11\,659\,191(59) \times 10^{-10}\,(\pm 5\,ppm)$ [10]. Combining all experimental data including the old CERN measurement, $a_\mu^{CERN} = 11\,659\,230(84) \times 10^{-10}\,(\pm 7.2\,ppm)$ [2], yields $a_\mu^{expt} = 11\,659\,205(46) \times 10^{-9}\,(\pm 4\,ppm)$ for the world average. This value agrees with the theoretical value $a_\mu^{SM} = 11\,659\,160(7) \times 10^{-10}\,(\pm 0.6\,ppm)$ found in [1].

4   Status of the Analysis of the 1999 and 2000 Data

The experiment currently analyses the data collected in 1999 which is about 15 times larger than the 1998 data set. In contrast to the old data, which could quite well be fitted to the basic 5-parameter function in equation (3), the significant increase in statistical power combined with a higher data taking rate revealed a number of subtle effects that slowed down the analysis. Two of the most prominent effects can be illustrated by ignorantly fitting the data to the function in eq. (3), and then looking at the residuals, i.e. the difference between the measured decay spectrum and the 5-parameter fit as shown in Fig. 4. Clearly the fitting function does not describe the data well. The residual in Fig. 4b,c has two prominent features. One is the excess of data at early times, and the other an oscillation of the counts with respect to the fitting function, also decaying with time. The former feature is caused by the high counting rate at early times. Our 400 MHz waveform digitizer does not allow us to distinguish between two decay positrons

that hit the same detector within about 3.5 nsec. Such pairs of pulses pile up to one larger pulse. If each of the single pulses exceed the energy threshold E, we lose a count. On the other hand, two pulses below threshold can combine to form a larger pulse that exceeds the threshold. Since our energy cuts are relatively high to benefit from the large asymmetry at higher energies, the pulses gained outnumber the pulses lost, leading to excessive counts at early times. An additional complication is that the g-2 phase of the pulses lost is not the same as the phase of the pulses gained because higher energy decay positrons have a larger bend radius in the ring magnet field and on average a longer flight path and flight time before hitting one of the calorimeters. Choosing an energy threshold where the pulses gained and pulses lost cancel does not eliminate the pile-up problem. As the muons decay, the count rate and therefore the fraction of pile-up pulses goes down. The simple 5-parameter fit to the data tries to accomodate the higher counts at early times by increasing the normalization constant, leading to an overestimate of counts at later times as seen in Fig. 4b.

An elegant way to extract the number of pile-up pulses from the data is to artificially increase the deadtime of the pulse finder by a factor of two, see how many more pulses are found above threshold, and then subtract these counts from the original decay positron spectrum. This sample of pulses can also be used to study the phase of the pile-up pulses. An alternative is to parametrize the pile-up fraction and include it in the fitting function. Both methods are used and compared in the analysis.

The oscillations in the residuals are caused by a coherent motion of the stored muon beam with a frequency that depends on the strength of the focusing electrostatic quadrupole field, the betatron tune. Due to a mismatch between the narrow inflector channel aperture, an 18 mm horizontal times 56 mm vertical rectangle, and the 90 mm diameter circular ring magnet aperture, we do not fill the available phase space in the storage ring in muon injection mode. This leads to a modulation of the horizontal beam width at the betatron oscillation frequency from the momentum spread, and a modulation of the horizontal and vertical beam width at twice this frequency from the angular spread of the incoming beam. In addition, our muon kicker runs reliably only a few percent below its design value. The resulting incomplete kick, combined with the fact that we do not fill the storage ring phase space, causes the beam centroid to oscillate about the central orbit at the betatron frequency. This coherent beam motion is known as coherent betatron oscillation or CBO. The dynamic behaviour of the stored muon beam was measured with a set of fiber harps that plunge in and out of the beam. Fig. 5 shows the motion of the beam centroid as an example.

The CBO is visible in the positron spectrum because the acceptance of our detectors is slightly dependent on the radius of the muon at the time of decay. The frequency we see is not the CBO frequency itself but its beating with the frequency of revolution, since we detect the decays at fixed points along the storage ring magnet circumference.

Other effects that need to be studied in detail include the loss of muons before they decay, the gain stability of the calorimeters and timing stability of the readout electronics, background events caused by the loss of protons that we inevitably store together with the muons, and background events called "flashlets". The flashlets are caused by a small
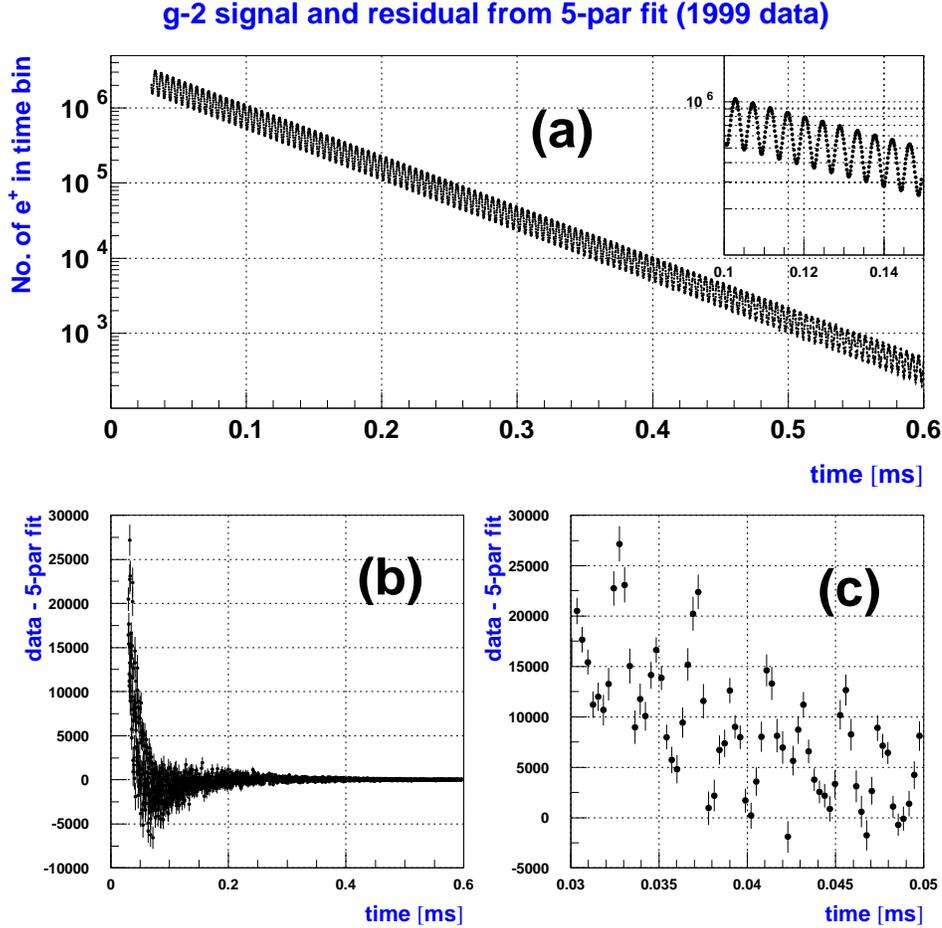
Figure 4: Positron spectrum from a large fraction of the 1999 data set (a), with an enlarged view of the time between 100 and 150 μsec after beam injection in the top right corner. The residuals from fitting the function in eq. (3) to the data show clear structure (b), particularly at early times (c).

fraction of the halo of the primary beam still circulating in the accelerator being scattered into the extraction line and transported to the production target. The resulting low intensity secondary beam does not get kicked and is therefore not stored in our ring magnet, but creates a small flash of background signals. The most troublesome secondary beam component is positrons. Starting with the momentum of the stored muon beam, the positrons spiral inwards due to energy loss in the inflector channel windows and give a signal that cannot be distinguished from true decay positron counts near the upper edge of the decay spectrum. We have developed a sensitive analysis method to detect these flashlets utilizing the discrete time structure associated with the 2.7 μsec revolution time of the beam in the accelerator. The flashlet contamination is very sensitive to the performance of the accelerator and we disregard data taken while there were elevated levels of flashlet contamination. During the 2000 run we installed a sweeper magnet in
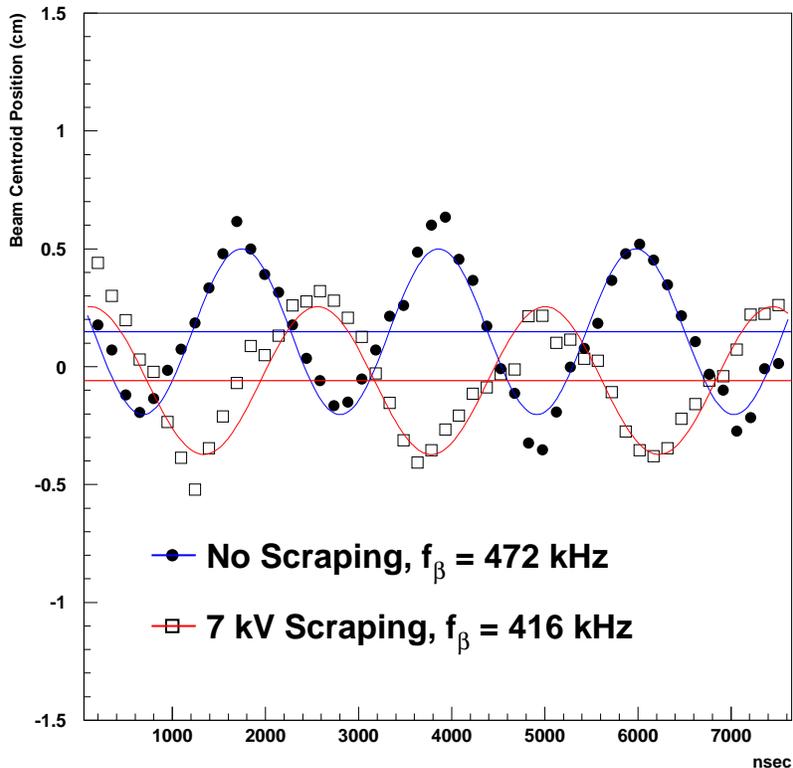
Figure 5: Beam centroid as measured by a set of fibers plunged into the muon beam at two different settings of the electrostatic quadrupoles. In normal running mode, the muon beam gets scraped for the first 15-20 μsec after injection by an imbalance in the quadrupole plate voltages which lowers the center of the electrostatic quadrupole field and therefore the beam centroid. This also changes the betatron tune.

the secondary beam line that turns on microseconds after beam injection into the storage ring and sweeps any late arrivals out of the beamline.

In the course of the data analysis all these effects have to be studied in detail, with different analysis teams developing their own tools to correct for them, parametrize them for inclusion into the fitting function, or estimate their impact on the fit parameters with analytical and Monte Carlo methods in cases where the unwanted or missing counts do not have unique characteristics but mix into other fitting parameters. This process is nearing completion for the 1999 data.

5 Future

The experiment is looking forward to another run from February through April 2001. Since the 2000 run we have reversed the polarity of the beam line and ring magnet to store negative muon beam and measure a_{μ^-}. We expect a decay positron rate similar to the 2000 run and hope to at least double our data set. Analysis of the 2000 data, 3-4 times larger than the 1999 data set, has started and initial checks e.g. for flashlet contamination suggest that most of the data is of good quality.

References

[1] A. Czarnecki and W.J. Marciano, **hep-ph/0010194**, these proceedings.

[2] J. Bailey et al., *Nucl. Phys.B.* **B150** (1979) 1.

[3] Particle Data Group, *Eur. Phys. J. C* **3** (1998) 1.

[4] W. Liu, et al., *Phys. Rev. Lett.* **82** (1999) 711.

[5] F. Krienen, et al., *Nucl. Instr. Meth. A.* **283** (1989) 5.

[6] G.D. Danby, et al., *Nucl. Instr. Meth. A* **457** (2001) 151.

[7] R. Prigl, et al., *Nucl. Instr. Meth. A.* **374** (1996) 118.

[8] X. Fei, et al., *Nucl. Instr. Meth. A.* **394** (1997) 349.

[9] R.M. Carey, el al., *Phys. Rev. Lett.* **82** (1999) 1632.

[10] H.N. Brown, el al., *Phys. Rev. D.* **62** (2000) 091101(R).